Journal of Luminescence 131 (2011) 1536–1540

Contents lists available at ScienceDirect

Journal of Luminescence

journal homepage: www.elsevier.com/locate/jlumin

Photoluminescence quenching of CdTe/CdS core-shell quantum dots in aqueous solution by ZnO nanocrystals

Aimin Shi [a,*], Jianhui Sun [b,c], Qinghui Zeng [b], Cong Shao [b,c], Zaicheng Sun [b], Haibo Li [d], Xianggui Kong [b], Jialong Zhao [b,**]

[a] School of Science, Dalian Jiaotong University, Dalian 116028, China
[b] Key Laboratory of Excited State Processes, Changchun Institute of Optics, Fine Mechanics and Physics, Chinese Academy of Sciences, 3888 Eastern South Lake Road, Changchun 130033, China
[c] Graduate School of Chinese Academy of Sciences, Beijing 100039, China
[d] Institute of Condensed Matter Physics and Materials Science, Jilin Normal University, Siping 136000, China

ARTICLE INFO

Article history:
Received 19 October 2010
Received in revised form
28 January 2011
Accepted 3 February 2011
Available online 19 February 2011

Keywords:
CdTe/CdS core-shell quantum dots
ZnO nanocrystals
Quantum confinement effect
Electron transfer
Photoluminescence quenching

ABSTRACT

Photoluminescence (PL) properties of 3-mercaptopropionic acid (MPA) coated CdTe/CdS core-shell quantum dots (QDs) in aqueous solution in the presence of ZnO colloidal nanocrystals were studied by steady-state and time-resolved PL spectroscopy. The PL quenching of CdTe/CdS core-shell QDs with addition of purified ZnO nanocrystals resulted in a decrease in PL lifetime and a small red shift of the PL band. It was found that CdTe(1.5 nm)/CdS type II core-shell QDs exhibited higher efficiency of PL quenching than the CdTe(3.0 nm)/CdS type I core-shell QDs, indicating an electron transfer process from CdTe/CdS core-shell QDs to ZnO nanocrystals. The experimental results indicated that the efficient electron transfer process from CdTe/CdS core-shell QDs to ZnO nanocrystals could be controlled by changing the CdTe core size on the basis of the quantum confinement effect.

© 2011 Elsevier B.V. All rights reserved.

1. Introduction

Colloidal semiconductor quantum dots (QDs) have gained great interest in fundamental research and technical applications such as light-emitting diodes (LEDs), photovoltaic cells, and sensors/detectors due to their size-dependent optical and electronic properties [1–5]. Recently, the charge transfer processes between QDs or between QDs and organic functional molecules were studied to understand the surface/interface properties of the QDs and to improve the performance of the QD-based devices by changing the shell materials and structures. The charge transfer processes are usually reflected by changes in the fluorescent properties of the QDs such as the variation of PL intensity and lifetime. Robel et al. [6] and Kongkanand et al. [7] confirmed electron injection from the excited state of CdSe QDs into TiO_2 nanoparticles by photoluminescence (PL) quenching and transient absorption spectra and found that the injection rate was dependent on the size of CdSe QDs and the functional molecules with different chains on the QD surface. Gross et al. [8] observed charge separation between type II aligned CdTe and CdSe nanocrystals. Recently Sudeep and Emrich [9] observed a pronounced PL quenching of CdSe core QDs upon introduction of the phosphine oxide functionalized Si QDs, suggesting photoexcited charge transfer from CdSe QDs to Si QDs. At the same time, we found that the efficiency of hole transfer from CdSe core-shell QDs with CdS, ZnS, and CdZnS shells to hole transporting materials by measuring PL quenching of CdSe QDs in the presence of hole transporting materials was related to the structures of the QD shell [10,11]. Generally, the shell as a passivating layer can improve the PL quantum yield (QY) and stability of QDs while it usually acts as a potential barrier to block the charge separation.

The PL QY and photostability of CdTe QDs as an important type of nanomaterials were improved dramatically by growing a CdS shell on the CdTe core [11–20]. CdTe/CdS core-shell QDs with a core of smaller than 1.5 nm in diameter were considered to be type II nanocrystals [19], in which the hole is mostly confined to the CdTe core, while the electron is mostly confined to the CdS shell due to their band offsets [17–20]. Consequently, the CdTe/CdS type II core-shell QDs may be used as efficient light-absorbing materials to fabricate photovoltaic devices because the band gap of CdTe QDs can be tuned with changing the particle size to match the solar spectrum well. On the other hand, ZnO material exhibits good electronic transport property, large carrier concentration

* Corresponding author. Tel.: +86 411 84106842.
** Corresponding author. Tel.: +86 431 86176029.
E-mail addresses: shiaimin@djtu.edu.cn (A. Shi), zhaojl@ciomp.ac.cn (J. Zhao).

0022-2313/$ - see front matter © 2011 Elsevier B.V. All rights reserved.
doi:10.1016/j.jlumin.2011.02.008

(about 10^{20} cm^{-3}), and high electron mobility (several tens of $cm^2\,V^{-1}\,s^{-1}$). Further, the overlap between the electronic states in CdTe QDs and the conduction band of the sensitized ZnO semiconductor will allow injection of electrons from CdTe QDs into ZnO, resulting in efficient separation of photogenerated charges. Therefore, it is necessary to explore the electron transfer process from CdTe QDs to ZnO by varying the size of CdTe QDs on the basis of quantum confinement effect.

In this work we report steady-state and time-resolved PL spectra of 3-mercaptopropionic acid (MPA) coated CdTe/CdS core-shell QDs with different core sizes in aqueous solution with the addition of as-prepared and purified ZnO colloidal nanocrystals. The PL quenching mechanisms of the CdTe/CdS core-shell QDs in the presence of the ZnO nanocrystals are discussed by the decrease in PL intensity and lifetime as well as the red shift of the PL band. Finally the improvement of electron transfer efficiency from CdTe/CdS core-shell QDs to ZnO nanocrystals is demonstrated by decreasing the CdTe core size on the basis of quantum confinement effect.

2. Experiment section

2.1. Synthesis of CdTe/CdS core-shell QDs

CdTe/CdS core-shell QDs in aqueous solution were synthesized via a method described in previously published procedure [19]. 20 mL of CdTe (0.1 mmol/L) QDs were added to a three-necked flask and stirred under Ar flowing for 1 h. Then the CdTe stock solution was heated up to 90 °C and the cadmium and sulfur injection solutions were dropped together into the solution at the speed of 0.1 mL/min. The cadmium injection solution (0.03 M) was prepared by dissolving $Cd(ClO_4)_2 \cdot 6H_2O$ and MPA in aqueous solution with the molar ratio MPA:Cd of 2.4. The sulfur injection solution (0.025 M) was prepared by dissolving $Na_2S \cdot 9H_2O$ in aqueous solution. The amount of Cd and S precursors required for one monolayer (ML) was determined by the number of the surface atoms of a given size of a core-shell QD. For example, in a typical experiment with 2 μmol of a 1.5 nm sized CdTe core, 2.8 mL of Cd and S precursors was needed for the first layer of the shell growth, and additional 3.6 mL of Cd and S precursors completed the growth of the second layer, and 5.0 mL of Cd and S precursors completed the growth of the third layer. The CdTe core size and CdS shell thickness were measured by transmission electron microscopy (TEM) in our previously published paper [19]. The MPA-coated CdTe/CdS core-shell QDs with CdTe cores of 1.5 and 3.0 nm diameter and a CdS shell of 3.0 ML labeled as CdTe(1.5 nm)/CdS and CdTe(3.0 nm)/CdS core-shell QDs were used in this experiment. Further, the QD samples were washed twice by dissolution in water and subsequent precipitation with methanol for removing excess ligands and other byproducts.

2.2. Synthesis of ZnO nanocrystals

The ZnO nanocrystals were synthesized using a modified method reported by Spanhel and Anderson [21]. The zinc complex precursor was prepared by refluxing ethanolic solution containing 0.1 M zinc acetate for 2–3 h. Next 10 mL of zinc complex precursor solution was diluted to 20 mL with ethanol. Further 117 mg (2.8 mmol) of $LiOH \cdot H_2O$ powder was added to the diluted ethanolic solution. The suspension was placed into an ultrasonic bath for 15 min at 40 °C in order to destroy the weakly soluble powder. Finally, the ZnO nanocrystals with an average diameter of 3.5 nm were obtained. To purify the ZnO nanocrystals, the as-prepared ZnO nanocrystals were washed twice by precipitation with n-hexane and dissolution in ethanol for removing excess Zn^{2+} and Li^{+} ions.

2.3. Steady-state and time-resolved fluorescence spectroscopy

The absorption spectra were recorded on a UV-3101PC UV–vis–NIR scanning spectrophotometer (Shimadzu). Steady-state PL spectra were recorded by a Hitachi F-4500 spectrophotometer. The time-resolved PL spectra were measured by FL920 fluorescence lifetime spectrometer (Edinburgh Instruments). The excitation source is a hydrogen flash lamp with a pulse width of 1.5 ns. All measurements were carried out at room temperature.

3. Results and discussion

Fig. 1 shows PL and absorption spectra of MPA-coated CdTe/CdS core-shell QDs with CdTe cores of 1.5 and 3.0 nm in diameter in aqueous solution. The PL spectra were taken at excitation wavelength of 400 nm. As seen in Fig. 1, the wavelength of the PL band for CdTe/CdS core-shell QDs is shifted to the red from 561 to 617 nm when the average diameter of the CdTe core is varied from 1.5 to 3.0 nm, which was determined by TEM. In comparison, the absorption spectrum of ZnO nanocrystals with an average diameter of 3.5 nm is also shown in this figure. The absorption onset of the ZnO nanocrystals is blue-shifted to about 345 nm, corresponding to an optical band gap of 3.6 eV, from the absorption wavelength (about 368 nm) of bulk ZnO due to quantum confinement effect. The full widths at half maximum (FWHM) of the PL bands of the CdTe/CdS core-shell QDs are estimated to be 48 and 65 nm, respectively. To study the charge transfer process between ZnO nanocrystals and CdTe/CdS core-shell QDs, in this experiment we selected the excitation wavelength of 400 nm that is below the band gap of 345 nm, which avoided the energy transfer process from ZnO nanocrystals to CdTe/CdS core-shell QDs [10,11].

The evolution of steady-state PL and absorption spectra of CdTe/CdS core-shell QDs in aqueous solution with addition of different concentrations of the purified ZnO nanocrystals from 0 to 1.76 mM is shown in Fig. 2. In the experiment, we fixed the absorbance of the two CdTe/CdS core-shell QD samples to the same value below about 0.1 of absorbance at excitation wavelength of 400 nm. As seen in Fig. 2(a), the PL intensity of

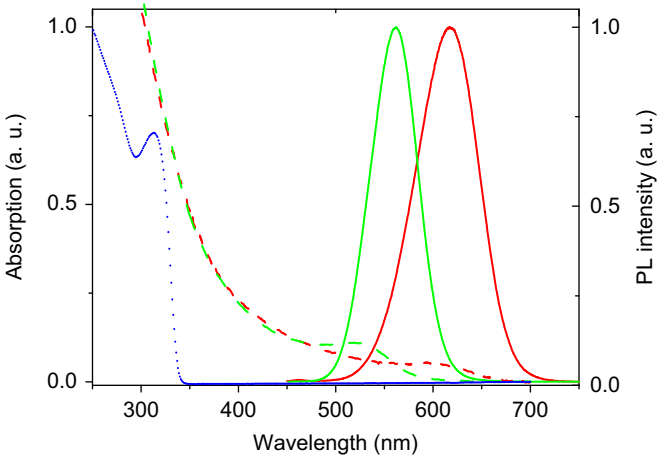

Fig. 1. PL and absorption spectra of CdTe/CdS core-shell QDs in aqueous solution. The solid (dashed) green and red lines represent PL (absorption) spectra of CdTe/CdS core-shell QDs with core diameters of 1.5 and 3.0 nm, respectively. The blue dotted line represents the absorption spectrum of ZnO nanocrystals. (For interpretation of the references to color in this figure legend, the reader is referred to the web version of this article.)

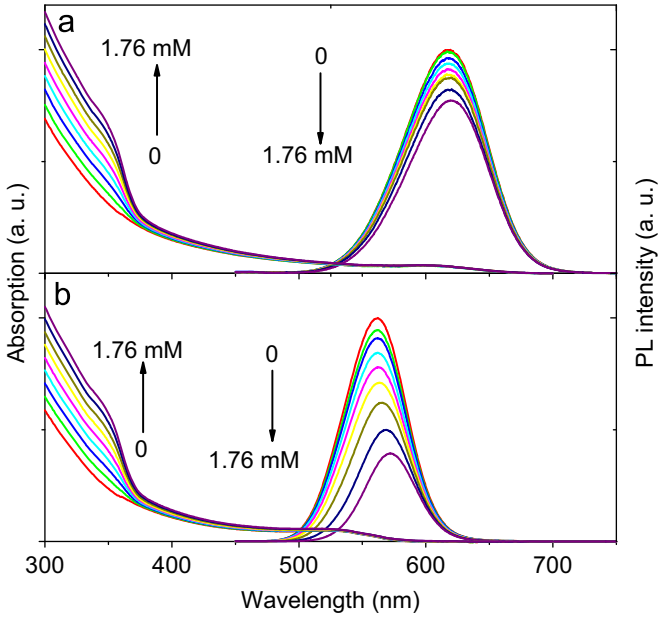

Fig. 2. PL and absorption spectra of CdTe/CdS core-shell QDs with CdTe core diameters of 3.0 nm (a) and 1.5 nm (b) in aqueous solution after addition of ZnO nanocrystals with different concentrations of 0, 0.22, 0.44, 0.66, 0.88, 1.10, 1.32, 1.54, and 1.76 mM.

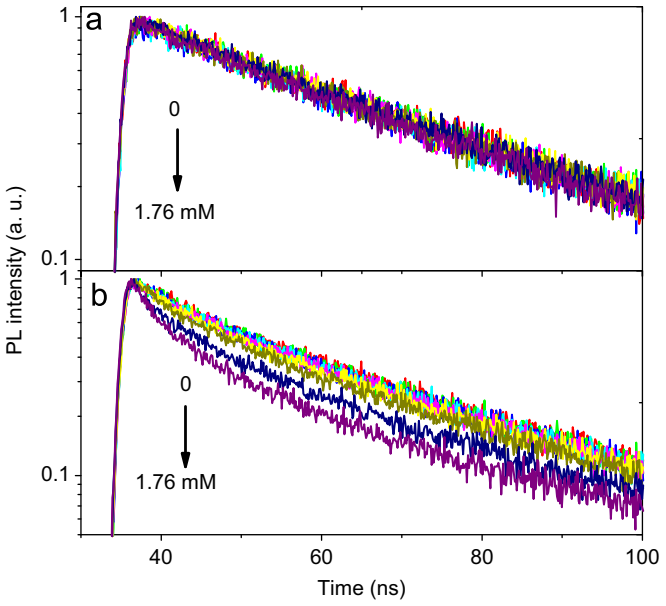

Fig. 3. PL decay curves of CdTe/CdS core-shell QDs with core diameters of 3.0 nm (a) and 1.5 nm (b) in aqueous solution after addition of ZnO nanocrystals with different concentrations of 0, 0.22, 0.44, 0.66, 0.88, 1.10, 1.32, 1.54, and 1.76 mM.

CdTe(3.0 nm)/CdS core-shell QDs is gradually decreased when the concentration of the ZnO colloidal nanocrystals added into the aqueous solution increased, causing the increase of the absorption above 345 nm. The PL band is slightly shifted to the red for about 2.0 nm when the concentration of ZnO colloidal nanocrystals is increased from 0 to 1.76 mM. Further, a significant PL quenching of the CdTe(1.5 nm)/CdS core-shell QDs is observed in Fig. 2(b) when ZnO colloidal nanocrystals with concentration from 0 to 1.76 mM is added into the aqueous solution. The PL band is significantly shifted to the red for about 10 nm. No significant absorption change was observed near the absorption edge of CdTe/CdS core-shell QDs. In addition, in order to understand the above red shift of the PL, we also measured the variation of PL spectra in CdTe/CdS core-shell QDs in the presence of as-prepared ZnO nanocrystals with large amount of Zn^{2+} ions. A PL quenching was clearly observed in both QD samples. However, the PL bands of CdTe(1.5 nm)/CdS and CdTe(3.0 nm)/CdS core-shell QDs were significantly shifted to the red for 20 and 32 nm, respectively. The large excitonic emission shifts of CdTe and CdSe QD solids with respect to the exciton peaks of the QDs in solution were previously explained by Forster energy transfer process [22–24]. Therefore, the significant PL red shift of the CdTe/CdS core-shell QDs by the addition of Zn^{2+} ions could be considered to come from the energy transfer process from CdTe/CdS core-shell QDs with a small core to the QDs with a large core. This indicated that the aggregation of differently sized CdTe/CdS core-shell QDs happened when ZnO nanocrystals in aqueous solution with large amount of Zn^{2+} ions was added into the CdTe/CdS core-shell QD solution. Therefore, the CdTe/CdS core-shell QDs exhibited more significant PL quenching and red shift than CdTe/CdS core-shell QDs in the presence of purified ZnO nanocrystals. In addition, the relatively red shift of the PL band also indicated that the CdTe/CdS core-shell QDs in aqueous solution had a relatively wide size distribution.

Fig. 3 shows the PL decay curves of the CdTe/CdS core-shell QDs in aqueous solution after the purified ZnO nanocrystals with different concentrations were added into the solution. The measurement was carried out at excitation wavelength of 400 nm. In order to study the decay process from the same QDs, the detection wavelengths were fixed at 561 and 617 nm for CdTe(1.5 nm)/CdS and CdTe(3.0 nm)/CdS core-shell QDs, respectively. As seen in Fig. 3(a), the PL lifetime is slightly decreased after adding the ZnO nanocrystals with various concentrations into the CdTe/CdS core-shell QD solution. Compared to CdTe(3.0 nm)/CdS core-shell QDs, the PL lifetime of the CdTe(1.5 nm)/CdS core-shell QDs is significantly shortened. These PL decay curves can be well fitted by a biexponential function described by an expression: $I(t)=A_1\exp(-t/\tau_1)+A_2\exp(-t/\tau_2)$, where τ_1 and τ_2 are the time constants and A_1 and A_2 represent the amplitudes of the components [19]. The average lifetime τ_{AV} is calculated by an expression $\tau_{AV}=(A_1\tau_1^2+A_2\tau_2^2)/(A_1\tau_1+A_2\tau_2)$. The fitting parameters A_1, A_2, τ_1, τ_2, and τ_{AV} are summarized in Tables 1 and 2. The PL lifetime of CdTe/CdS core-shell QDs is significantly decreased with increasing ZnO nanocrystal concentration.

Table 1
Time constants, amplitudes, and average lifetimes for the CdTe(3.0 nm)/CdS core-shell QDs with various ZnO nanocrystal concentrations.

Concentration (mM)	Parameter				
	τ_1 **(ns)**	A_1	τ_2 **(ns)**	A_2	τ_{AV} **(ns)**
0	11.22	0.442	24.10	0.558	**20.63**
0.22	11.34	0.455	24.24	0.545	**20.62**
0.44	11.84	0.504	24.85	0.496	**20.60**
0.66	10.97	0.440	23.94	0.560	**20.50**
0.88	11.39	0.460	24.17	0.540	**20.51**
1.10	10.27	0.411	23.53	0.589	**20.43**
1.32	9.87	0.404	23.48	0.596	**20.46**
1.54	9.81	0.410	23.31	0.590	**20.26**
1.76	8.39	0.387	22.99	0.613	**20.26**

The ratios of PL intensity (I_0/I) and average lifetime (τ_{AV0}/τ_{AV}) of the CdTe/CdS core-shell QDs as a function of the purified ZnO nanocrystal concentration are shown in Fig. 4. The subscript 0 denotes the parameters (PL intensity or lifetime of the QDs) in the absence of the ZnO nanocrystals. As is well known, majority of PL

Table 2
Time constants, amplitudes, and average lifetimes for the CdTe(1.5 nm)/CdS core-shell QDs with various ZnO nanocrystal concentrations.

Concentration (mM)	Parameter				
	τ_1 **(ns)**	A_1	τ_2 **(ns)**	A_2	τ_{AV} **(ns)**
0	4.254	0.268	25.52	0.733	**24.30**
0.22	5.507	0.298	25.54	0.702	**23.86**
0.44	4.729	0.303	25.91	0.697	**24.35**
0.66	3.922	0.303	24.18	0.697	**22.84**
0.88	4.440	0.313	24.22	0.687	**22.69**
1.10	4.897	0.365	23.36	0.635	**21.37**
1.32	4.202	0.414	24.94	0.586	**20.79**
1.54	2.743	0.491	20.56	0.509	**18.52**
1.76	2.955	0.602	19.86	0.398	**16.75**

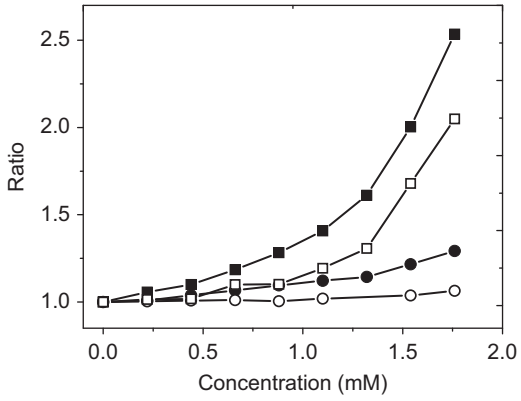

Fig. 4. I_0/I (solid squares and circles) and τ_{AV0}/τ_{AV} (empty squares and circles) ratios of CdTe/CdS core-shell QDs with the core diameters of 1.5 (squares) and 3.0 nm (circles) as a function of ZnO nanocrystal concentration.

quenching results are explained by the Stern–Volmer equation $I_0/I=1+K_{SV}[Q]$, where K_{SV} is the Stern–Volmer constant and [Q] is concentration of quencher [25,26]. However, the plots of I_0/I versus quencher concentration in this experiment do not fit this conventional linear Stern–Volmer equation. The plots in Fig. 4 indicate that both dynamic and static quenching processes occur in the CdTe/CdS–ZnO nanomaterial system or there are multiple PL pathways with different quenching efficiencies [27–30]. Moreover, the relationship between the lifetime quenching ratio and ZnO nanocrystal concentration is also nonlinear. This means that the PL quenching comes not only from the dynamic quenching that has a contribution of electron transfer from CdTe/CdS core-shell QDs to ZnO nanocrystals but also from the static quenching that is related to the decrease of emitting centers in CdTe/CdS core-shell QDs [10]. Further, the quenching ratio of τ_{AV0}/τ_{AV} for the CdTe(1.5 nm)/CdS core-shell QDs is slightly smaller than that of its PL intensity. Therefore, we hypothesize that the PL quenching is mainly caused by electron transfer from photoexcited CdTe/CdS core-shell QDs to the ZnO nanocrystals. On the basis of the variation in the PL intensity (or lifetime), the efficiencies of the PL quenching, $E=1-I_0/I$ (or $E=1-\tau_{AV0}/\tau_{AV}$), for CdTe/CdS core-shell QDs with core diameters of 3.0 and 1.5 nm in the presence of the purified ZnO nanocrystals with a concentration of 1.76 mM were estimated to be 23% (6%) and 61% (51%), respectively. Therefore, the CdTe/CdS core-shell QDs with a smaller CdTe core exhibit highly efficient PL quenching, indicating an efficient electron transfer process from CdTe/CdS core-shell QDs with a small core to the ZnO nanocrystals due to quantum confinement effect.

As is known above, MPA-coated QDs are easily tethered to the surface of ZnO nanocrystals with –COOH groups. The transfer of the photoexcited electrons in the CdTe/CdS core-shell QDs into the ZnO nanocrystals can quench the PL intensity and lifetime of the QDs, depending on the structure of CdTe/CdS core-shell QDs such as the core size and QD structure. Fig. 5 shows the schematic diagram of electronic levels and structures of the CdTe/CdS type I and type II core-shell QDs and ZnO nanocrystals. The dynamic PL quenching of the CdTe/CdS core-shell QD can be explained by electron transfer from CdTe/CdS core-shell QDs to ZnO nanocrystals. From previous experimental results, CdTe/CdS core-shell QDs with the core of 1.5 and 3.0 nm diameter were suggested to be type II and I nanocrystals, respectively [17–20]. For the type I QDs, the CdS shell is a potential barrier to block the transfer of photoexcited electrons in CdTe cores to ZnO nanocrystals as shown in Fig. 5(a), while for type II QDs, the CdS shell is not a potential barrier but a bridge. Therefore, photoexcited electrons in CdTe cores are first transferred to CdS shell and then to ZnO nanocrystals, resulting in an efficient PL quenching as shown in Fig. 5(b). We found the significant PL quenching of CdTe(1.5 nm)/CdS core-shell QDs caused a lager PL red shift (10 nm) than that (2 nm) of CdTe(3.0 nm)/CdS core-shell QDs when the purified ZnO nanocrystals were added to the aqueous solutions. This means that CdTe/CdS type II core-shell QDs with a smaller core exhibit more efficient electron transfer to the ZnO nanocrystals, greatly quenching their PL. Therefore, the PL band of CdTe(1.5 nm)/CdS was shifted to the red wavelength due to a relatively wide core size and shell thickness distribution of the CdTe/CdS core/shell QDs.

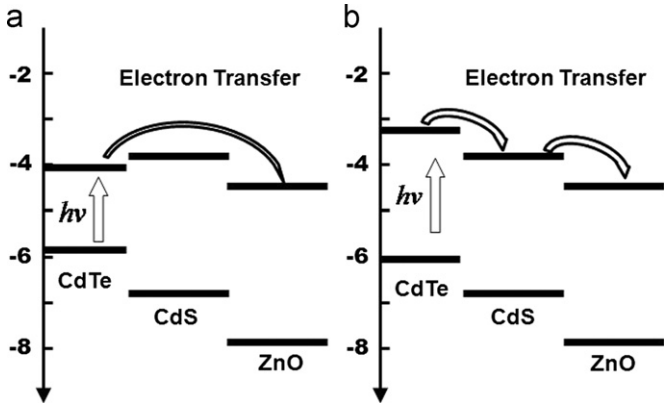

Fig. 5. Schematic diagrams of electron transfer processes for CdTe/CdS type I (a) and type II (b) core-shell QDs from CdTe cores to ZnO nanocrystals. The electronic level structures of the CdTe/CdS core-shell QDs and ZnO nanocrystals are taken from previous data [19,30].

4. Conclusions

In summary, we have demonstrated that the electron transfer process from CdTe/CdS core-shell QDs to ZnO nanocrystals results in an efficient PL quenching of the CdTe QDs. The efficiency of the electron transfer was improved by decreasing the size of the CdTe core to make CdTe/CdS core-shell QDs become type II QDs on the basis of the quantum confinement effect. It is expected that the efficiency can be further enhanced by controlling the electronic interaction between CdTe/CdS core-shell QDs and ZnO nanocrystals or synthesizing the QDs with a narrow size distribution. Therefore, highly efficient electron transfer process from CdTe/CdS core-shell QDs to ZnO nanocrystals will significantly improve the performance of the QDs based solar cells.

Acknowledgments

This work was supported by the program of CAS Hundred Talents, the National Natural Science Foundation of China

(nos. 10874179, 10904142, 60976049, 11004188, and 60671015). We thank Dr. Xiuying Wang for her helpful discussion.

References

[1] S. Coe, W.K. Woo, M. Bawendi, V. Bulovic, Nature 420 (2002) 800.
[2] J.L. Zhao, J.A. Bardecker, A.M. Munro, M.S. Liu, Y.H. Niu, I.K. Ding, J.D. Luo, B.Q. Chen, A.K.Y. Jen, D.S. Ginger, Nano Lett. 6 (2006) 463.
[3] Q. Sun, Y.A. Wang, L. Li, D. Wang, T. Zhu, J. Xu, C. Yang, Y. Li, Nat. Photon. 1 (2007) 717.
[4] W.U. Huynh, J.J. Dittmer, A.P. Alivisatos, Science 295 (2002) 2425.
[5] D.V. Talapin, J. Lee, M.V. Kovalenko, E.V. Shevchenko, Chem. Rev. 110 (2010) 389.
[6] I. Robel, V. Subramanian, M. Kuno, P.V. Kamat, J. Am. Chem. Soc. 128 (2006) 2385.
[7] A. Kongkanand, K. Tvrdy, K. Takechi, M. Kuno, P.V. Kamat, J. Am. Chem. Soc. 130 (2008) 4007.
[8] D. Gross, A.S. Susha, T.A. Klar, E.D. Como, A.L. Rogach, J. Feldmann, Nano Lett. 8 (2008) 1482.
[9] P.K. Sudeep, T. Emrick, ACS Nano 3 (2009) 4105.
[10] Y.L. Zhang, P.T. Jing, Q.H. Zeng, Y.J. Sun, H.P. Su, Y.A. Wang, X.G. Kong, J.L. Zhao, H. Zhang, J. Phys. Chem. C 113 (2009) 1886.
[11] Y.L. Zhang, X.G. Kong, Y.Q. Qu, P.T. Jing, Q.H. Zeng, Y.J. Sun, Y.A. Wang, J.L. Zhao, H. Zhang, J. Lumin. 129 (2009) 1410.
[12] H.B. Bao, Y.J. Gong, Z. Li, M.Y. Gao, Chem. Mater. 16 (2004) 3853.
[13] Y. He, H.T. Lu, L.M. Sai, W.Y. Lai, Q.L. Fan, L.H. Wang, W. Huang, J. Phys. Chem. B 110 (2006) 13370.
[14] C.L. Wang, H. Zhang, J.H. Zhang, M.J. Li, H.Z. Sun, B. Yang, J. Phys. Chem. C 111 (2007) 2465.
[15] B. Schreder, T. Schmidt, V. Ptatschek, U. Winkler, A. Materny, E. Umbach, M. Lerch, G. Muller, W. Kiefer, L. Spanhel, J. Phys. Chem. B 104 (2000) 1677.
[16] J. Wang, Y.T. Long, Y.L. Zhang, X.H. Zhong, L.Y. Zhu, Chem. Phys. Chem. 10 (2009) 680.
[17] O. Scho1ps, N.L. Thomas, U. Woggon, M.V. Artemyev, J. Phys. Chem. B 110 (2006) 2074.
[18] J.Y. Chang, S.R. Wang, C.H. Yang, Nanotechnology 18 (2007) 345602.
[19] Q.H. Zeng, X.G. Kong, Y.J. Sun, Y.L. Zhang, L.P. Tu, J.L. Zhao, H. Zhang, J. Phys. Chem. C 112 (2008) 8587.
[20] D. Dorfs, T. Franzl, R. Osovsky, M. Brumer, E. Lifshitz, T.A. Klar, A. Eychmuller, Small 4 (2008) 1148.
[21] L. Spanhel, M.A. Anderson, J. Am. Chem. Soc. 113 (1991) 2826.
[22] S.F. Wuister, R. Koole, C. de M. Donega, A. Meijerink, J. Phys. Chem. B 109 (2005) 5504.
[23] C.R. Kagan, C.B. Murray, M. Nirmal, M.G. Bawendi, Phys. Rev. Lett. 76 (1996) 1517.
[24] S.A. Crooker, J.A. Hollingsworth, S. Tretiak, V.I. Klimov, Phys. Rev. Lett. 89 (2002) 186802.
[25] C. Landes, C. Burda, M. Braun, M.A. El-Sayed, J. Phys. Chem. B 105 (2001) 2981.
[26] O. Schmelz, A. Mews, T. Basche, A. Herrmann, K. Mullen, Langmuir 17 (2001) 2861.
[27] Al.L. Efros, M. Rosen, M. Kuno, M. Nirmal, D.J. Norris, M.G. Bawendi, Phys. Rev. B 54 (1996) 4843.
[28] S.F. Wuister, C.M. Donega, A. Meijerink, J. Phys. Chem. B 108 (2004) 17393.
[29] O. Schops, N.L. Thomas, U. Woggon, M.V. Artemyev, J. Phys. Chem. B 110 (2006) 2074.
[30] C.G. Van de Walle, J. Neugebauer, Nature 423 (2003) 626.